

Fabrication of two-dimensional photonic crystals with controlled defects by use of multiple exposures and direct write

Lin Pang, Wataru Nakagawa, and Yeshaiahu Fainman

We have developed an approach for relatively rapid and easy fabrication of large-area two-dimensional (2-D) photonic crystal structures with controlled defects in the lattice. The technique is based on the combination of two lithographic steps in UV-sensitive SU-8 photoresist. First, multiple exposures of interference fringes are used in combination with precise rotation of the sample to define a 2-D lattice of holes. Second, a strongly focused UV laser beam is used to define line-defect waveguides by localized exposure in the recorded but not yet developed lattice from the first step. After development, the mask is transferred into a GaAs substrate with dry etching in chemically assisted ion-beam etching. © 2003 Optical Society of America

OCIS codes: 230.4000, 090.0090, 250.5300, 130.3120.

1. Introduction

Photonic crystals hold great promise for the realization of integrated photonic circuits as they provide a platform on which numerous useful photonic devices (e.g., waveguides, resonators, detectors, optical sources, and nonlinear optical elements) can be produced with compatible materials and fabrication technologies. However, for this potential to be fully realized, it is necessary to reduce the complexity of fabrication of various photonic elements, such that rapid and inexpensive manufacturing of large-scale integrated photonic systems can be achieved.

At present, most photonic crystals are fabricated by one of three manufacturing techniques. In the first technique, self-assembly of microspheres or other basic structures are used.^{1,2} In the second technique, optical interferometric patterning of photoresist is used with multiple coherent beams.³⁻⁷ Both of these approaches have been successfully demonstrated, producing large-area photonic crystal structures in both two and three dimensions. However, to employ

a photonic crystal lattice as an integration platform to manufacture functional optical components and subsystems, it will be necessary to develop techniques that can produce locally controlled variations or defects in the photonic crystal lattice. Multiphoton polymerization was used to produce waveguide structures in self-assembled three-dimensional opal; however, the alignment of the defects in the lattices still needs to be improved.⁸ Consequently, most of the photonic crystal-based devices have been patterned by use of the third approach that is based on E-beam lithography^{9,10} in which design flexibility and control of the structure can be achieved with a high degree of precision. However, in comparison with the self-assembled or interferometric approaches, the direct-write E-beam lithography method is an extremely slow and expensive process, making it largely impractical for the manufacture of large integrated photonic systems.

In this paper we describe an approach to manufacture photonic crystal-based devices using a two-step process consisting of interferometric patterning to define the photonic crystal lattice followed by optical direct write of the functional elements. First, the photonic crystal lattice is patterned in photoresist by interferometric optical lithography, producing a large-area (approximately 1 cm²) lithographic pattern quickly and easily. In the second step, the variations or defects in the lattice to implement the functional devices are created by optical direct write with a strongly focused optical beam. After the pat-

The authors are with the Department of Electrical and Computer Engineering, University of California, San Diego, 9500 Gilman Drive, La Jolla, California 92093-0407. The e-mail address for L. Pang is lpang@ece.ucsd.edu.

Received 6 March 2003; revised manuscript received 23 May 2003.

0003-6935/03/275450-07\$15.00/0

© 2003 Optical Society of America

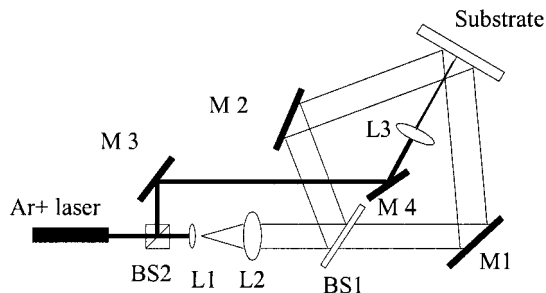


Fig. 1. Schematic of the two-beam interferometric lithography for fabrication of a 2-D photonic crystal. The laser beam is expanded by L1 (a UV objective lenses with focal length of 11.5 mm), collimated by UV lens L2 with a focal length of 100.0 mm, and is split into two equal intensity beams after beam splitter BS1 and then is recombined on the resist that is coated on the substrate. Beam splitter BS2 is used to obtain a scanning beam exposing the resist by a reflective MO lens L3, 36 \times (numerical aperture of 0.52) with a focal length of 10.4 mm (from Thermo Oriel).

tering processes, the mask is developed and a dry-etching process is used to transfer the desired pattern into a high-dielectric-constant GaAs substrate. Because the entire large-scale photonic crystal lattice is essentially created at once with the interferometric patterning approach, the direct-write process is needed only to implement the functional elements (e.g., waveguides, cavities) instead of the entire lattice. Thus this hybrid approach possesses an advantage in terms of fabrication time and cost as compared with E-beam lithography for the patterning of large-scale photonic crystal-based integrated systems.

This paper is structured as follows. In Section 2 we describe the interferometric patterning process to create the photonic crystal lattice for both square and hexagonal lattice structures. In Section 3 we present an example of the optical direct-write method to produce a line defect for implementing a straight waveguide in a photonic crystal lattice. Finally, in Section 4 we present a discussion and our conclusion.

2. Interferometric Lithography and Fabrication of a Two-Dimensional Photonic Crystal

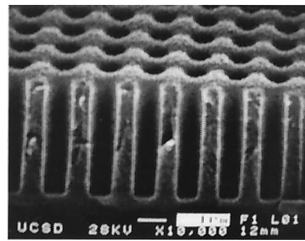
The first step in our fabrication process is to create a large-scale photonic crystal lattice using an optical interference pattern. For this purpose, an Ar⁺ ion laser operating at a wavelength of 364 nm is used as the illumination source of the UV-sensitive SU-8 negative chemically amplified photoresist. The beam from the laser is expanded and collimated and then split into two beams with a nonpolarizing UV beam splitter (see Fig. 1). The two beams are then reflected onto the sample at an angle that can be adjusted to achieve the desired period: $\lambda/[2 \sin(\theta/2)]$, where λ and θ are the wavelength of the laser and the angle between the two beams, respectively. The resulting intensity pattern is sinusoidal and has been used in the past to generate one-dimensional grating structures in UV-sensitive photoresist spun on various substrates. In our setup the substrate is

mounted on a high-precision translation-rotation stage. The in-plane substrate rotation allows for multiple exposure of the photoresist to the one-dimensional interference pattern, producing two-dimensional (2-D) periodic structures. By proper choice of the rotation angles, exposure doses, and type of the UV photoresist (positive or negative), we can generate different structures and shapes in the resist after development. The 2-D periodic structures defined and fabricated in photoresist can easily be transferred into high-refractive-index materials, such as GaAs or Si, by use of standard dry-etching techniques.

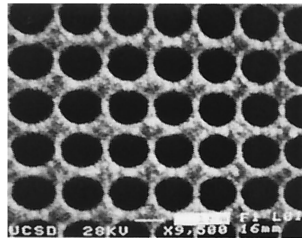
Interferometric optical lithography differs from conventional optical lithography in the intensity profile in the volume of the photoresist as well as the thickness of the photoresist used. In the former case, the intensity distribution is sinusoidal because of the interference characteristics; however, with standard optical lithography it is nearly rectangular when a mask aligner or a stepper is used to expose thin layers of photoresist. Furthermore, with the interferometric optical lithography technique, the thickness of the photoresist can be optimized to meet the needs of the etching processes. On the basis of our recent investigation and experience with the fabrication of optical devices in SU-8 (MicroChem Corp.),¹¹ we select it for our current study on the fabrication of 2-D photonic crystals. SU-8 is a chemically amplified negative resist, which consists of three components: an epoxy resin, a solvent, and a photoacid generator (photoinitiator). Exposure to UV light (as well as x rays or energetic electrons) generates induced acid (i.e., Lewis acid) in the latent image. A postexposure bake (PEB) at a higher temperature than the glass transition temperature ($\sim 55^\circ\text{C}$) is then used to catalyze the formation of cross-linking through a cationic photoamplification mechanism. Subsequent development of the film dissolves the unexposed regions, leaving behind the cross-linked material. SU-8 has high optical transparency above 360 nm, making it ideally suited to achieve vertical sidewalls in thick films.¹² In our experiments, the SU-8 resist is spin coated on cleaned substrates, where the thickness of the SU-8 layer on the substrate is controlled by the spinning speed. Before illumination, a soft bake process is performed at a temperature of 95°C for 10 min to remove all the solvent in the SU-8 layer. After the illumination, the sample is baked in an oven, corresponding to a PEB step to perform cationic photopolymerization of the epoxy. The SU-8 is then developed in propylene glycol methyl ether acetate, with the development time depending on the thickness of the layer. After development, the sample is rinsed in a solvent of isopropyl alcohol and then dried in air.

A. Fabrication of a Two-Dimensional Photonic Crystal with Square and Hexagonal Lattice Structures

The sinusoidal distribution of the interference pattern and the exposure mechanism of the chemically amplified resist will have a strong influence on the



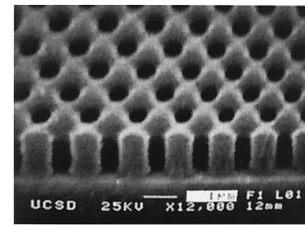
(a)



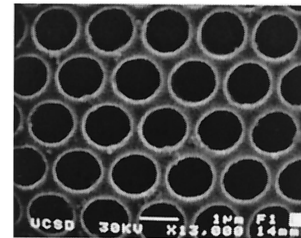
(b)

Fig. 2. Experimental results of the fabrication of a rectangular mesh photonic crystal lattice produced by double exposure of SU-8 by use of an interference pattern oriented in two orthogonal directions. The SEM photographs of the obtained square lattice with a period of $1.5 \mu\text{m}$ show that the diameter of the fabricated holes can be controlled by the exposure density producing (a) small holes with a diameter of $0.9 \mu\text{m}$ obtained with an exposure of approximately $30 \text{ mJ}/\text{cm}^2$ for a 1-min bake time in PEB and (b) large holes with a diameter of $1.3 \mu\text{m}$ with an exposure of $15 \text{ mJ}/\text{cm}^2$ for 2 min in PEB.

resultant profile in the SU-8 resist. The exposure dosage as well as the PEB will play a major role in the determination of the structure of the fabricated photonic crystal lattices; furthermore, the combination of an adjustment of the exposure time and the PEB will produce the desired profile.¹¹ We used our past experience and developed an exposure optimization methodology for fabrication procedures to construct 2-D periodic structures. Our first example of fabrication of 2-D periodic structures is a rectangular mesh photonic crystal lattice. The photoresist on the GaAs substrate is double exposed to the same interference pattern, with the second exposure occurring after the substrate was rotated in plane by 90° . Figure 2(a) shows a scanning electron microscopy (SEM) image of such a square periodic structure with a $1.5\text{-}\mu\text{m}$ period. With exposures of approximately $30 \text{ mJ}/\text{cm}^2$ and a measured layer thickness of approximately $4.4 \mu\text{m}$, we observe a hole diameter of $0.9 \mu\text{m}$. In fact, we successfully produced 2-D square periodic structures with a $0.5\text{-}\mu\text{m}$ period in photoresist layers of up to $11 \mu\text{m}$ thick. Furthermore, it is easy to change the period of the lattice and the diameter of the holes by means of adjusting such parameters as the angle between the two interfering beams, the exposure dosage, the bake time, and the temperature used during the PEB step.¹¹ Figure 2(b) shows a sample with an increased hole diameter of $1.3 \mu\text{m}$ with the same period of $1.5 \mu\text{m}$ produced when the exposure is decreased to approximately 15



(a)



(b)

Fig. 3. Experimental results of the fabrication of a hexagonal photonic crystal lattice produced by triple exposure of SU-8 by use of an interference pattern rotated by 60° between each exposure. The SEM photographs of the obtained hexagonal lattice with a period of $1.5 \mu\text{m}$ show that (a) small holes with a diameter of $0.7 \mu\text{m}$ are obtained with exposure of approximately $28 \text{ mJ}/\text{cm}^2$ for a 1-min bake time in PEB and (b) large holes with a diameter of $1.1 \mu\text{m}$ are obtained with an exposure of approximately $10 \text{ mJ}/\text{cm}^2$ for 2 min in PEB.

mJ/cm^2 and the bake time is increased in the PEB step to 2 min.

The reproducibility of the experimental results depends on the stability of the processing parameters, including variations in the laser output and undulation of the temperature in the oven and developer. In our experiment, the results are not dependent on the above environmental factors because of the stability of the Ar^+ laser and the baking oven, as well as the low temperature sensitivity of high-contrast SU-8 resist. The only remaining factor is the uniformity of the intensity distribution of the laser beam, which would affect the uniformity of the lattice structure. By expanding the laser beam and selecting its central part, we can obtain uniform exposure over the area of interest.

B. Fabrication of the Hexagonal Lattice and the Alignment in Three Exposures

A hexagonal 2-D photonic crystal lattice can be similarly produced in SU-8, but we have to expose the substrate three times to the same interference pattern with in-plane substrate rotations of 60° and 120° . Figure 3(a) presents a structure with a $1.5\text{-}\mu\text{m}$ period in a layer of photoresist with a thickness of $1.3 \mu\text{m}$. With a total exposure of approximately $28 \text{ mJ}/\text{cm}^2$, we measured a hole diameter of $0.7 \mu\text{m}$. Figure 3(b) is a top view of another sample with the same structure but made with a slightly decreased exposure of approximately $10 \text{ mJ}/\text{cm}^2$ and increased bake time of 2 min in the PEB process,

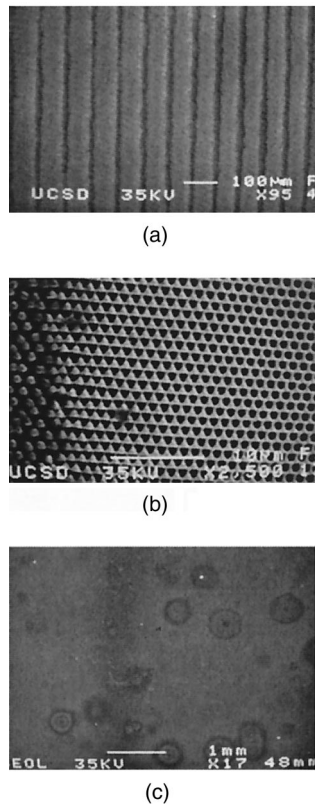


Fig. 4. SEM photographs of a hexagonal lattice structure in SU-8 to show the beat period that is due to the misalignment of the substrate rotations: (a) result from use of a manually controlled rotation stage; (b) magnified transition areas in (a); (c) result obtained with a high-precision Physik Instrumente rotating stage with perfect hole areas approximately 2 mm wide.

producing holes with an increased diameter of 1.1 μm .

It should be noted that accurate alignment of the three exposures is critical to produce a high-quality, large-area hexagonal photonic crystal pattern. If the vector sum of the grating wave vectors for each interferometric exposure is not zero, because of a deviation of either the grating period or the angular orientation, then a spatial beat frequency will result. Consequently, the resulting exposed pattern in the resist will vary across the sample, with a characteristic length corresponding to the spatial beat frequency, and this will effectively limit the usable area of the sample. With a manually controlled rotation stage, the inaccuracy in the angular alignment of the three exposures results in a spatially varying pattern with a period of approximately 70 μm , as shown in Figs. 4(a) (wide view) and 4(b) (magnified view). In some areas [e.g., the lighter areas in Fig. 4(a) or the right side of Fig. 4(b)] well-defined circular holes are produced as intended. However, in other areas [e.g., the darker areas in Fig. 4(a) or the center and left side of Fig. 4(b)] the shapes of the holes change from nearly perfect circles to triangles and eventually to a completely unusable pattern. For this sample, the usable area with perfect circular holes is only approx-

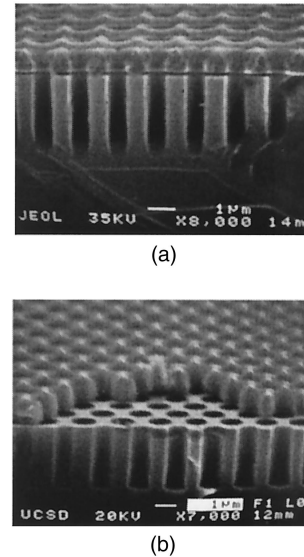


Fig. 5. SEM micrograph of 2-D photonic crystals with period of 1.5 μm transferred into a GaAs substrate by CAIBE: (a) orthogonal lattice with a 3- μm depth in a GaAs substrate; (b) a hexagonal periodic structure with a 3- μm depth.

imately 30 μm wide, validating the approach but providing unsatisfactory results for the ultimate goal of large-scale integration. However, by improving the alignment accuracy in the exposure process, we can obtain a significantly larger hexagonal lattice photonic crystal pattern. Using a high-precision computer-controlled rotation stage (Physik Instrumente Model M-037.PD), we can increase the characteristic length of the misalignment of the three exposures to approximately 4 mm. This results in a sample having a usable area with the desired photonic crystal pattern of approximately 2 mm \times 10 mm, as shown in Fig. 4(c). The spots in Fig. 4(c) are due to particles in the resist. The usable area can be easily cut for practical use and could be further enlarged with even greater accuracy in the rotation stage.

C. Transferring from the SU-8 Resist into High-Index Substrates with Dry Etching

Because of its low refractive index of approximately 1.6 at a 1.55- μm wavelength, the structures in SU-8 cannot be used as a photonic crystal device with broad bandgap characteristics. Therefore it is desirable to transfer the patterns recorded and developed in SU-8 into high-index substrates, such as GaAs. For this purpose, the GaAs wafer with the fabricated SU-8 mask was directly placed into the chamber of a chemically assisted ion-beam etching (CAIBE) system. In CAIBE, Cl_2 is used as a chemical etching gas. The etching rate and profile are influenced by many parameters in the system, such as beam voltage, accelerator voltage, beam current, and gas flow of Cl_2 . With optimized dry-etching parameters, a vertical sidewall etched profile was achieved. Figure 5(a) shows the etched orthogonal structure with period of 1.5 μm and a depth of approximately 3.0 μm

with the SU-8 layer as the dry-etching mask. The erosion rate of the resist and the etching rate of GaAs are 5 and 16 nm/min, respectively, such that the etching rate selectivity is approximately 3:1. With the above etching parameters, it is possible to transfer the hexagonal periodic pattern into the GaAs substrate as shown in Fig. 5(b) where the depth is approximately 3 μm with a 1.5- μm period. It can be seen that there is some SU-8 residue on the substrate after the dry etching; with thicker masks, even deeper structures can be achieved.

With the multiple-exposure approach, a large-area 2-D photonic crystal lattice can be patterned quickly and easily. However, the greatest advantage of this technique lies in the fact that, after the photonic crystal lattice is patterned, the photoresist layer is still photosensitive and can be further processed. Thus desired modifications in the lattice pattern can be produced with additional selective exposure of the photoresist. In Section 3 we describe the second step in our approach, the creation of a simple functional structure in the optically patterned photonic crystal lattice: a straight waveguide consisting of several missing rows of holes.

3. Introducing Defects by Direct Write with a Strongly Focused Beam

The negative photoresist nature of SU-8 allows for further modification of the exposed photonic crystal lattice by selective point-by-point exposure of areas that have not yet been exposed. Such a process can be used to introduce point defects to create 2-D nanocavities, line defects to create a linear waveguide, as well as any desired pattern in principle. For realization of the photonic lattice modification, we employ a high-precision translation stage (Physik Instrumente Model M-224.20) to control the position where the defect will be introduced. To achieve high resolution for direct write of the line defect, we employ a 36 \times reflective microscope objective (MO) (numerical aperture of 0.52) with a focal length of 10.4 mm (from Thermo Oriol).

We next perform the calibration of our direct-write approach by investigating the effect of the deposited exposure energy on the width of the resulting defect in SU-8. When we use the fixed PEB process parameters of a 60-s bake time at 90 $^{\circ}\text{C}$, the width of the obtained line in SU-8 depends only on the exposure dose, which in turn is a function of the incident intensity and the scanning speed. For simplicity, we also set the scanning speed to be constant at approximately 0.3 mm/s, such that the linewidth will depend only on the incident intensity as shown in Fig. 6, which shows the square of the linewidth as a function of a logarithmic scale for the intensity. It is expected that a square of the linewidth of the scanned lines would be a linear function of the logarithmic intensity if the linewidth results only from the spot size of the focused beam with a Gaussian intensity distribution. However, the data in Fig. 6 show different characteristics in the small and large feature size regions. In the large feature size region, with

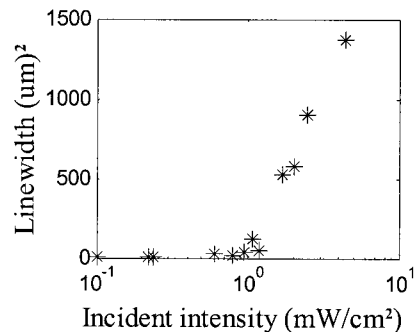


Fig. 6. Dependence of width of the scanned line in SU-8 on incident intensity by a 36 \times reflective MO with the square of the linewidth as a function of the intensity on logarithmic scale.

decreasing intensity from approximately 4.0 to 1 mW/cm², the linewidth decreases rapidly from approximately 37 to 6 μm . Then, in the small feature size region, the linewidth decreases slowly from approximately 4 to 2 μm when the intensity is decreased from approximately 0.8 to 0.2 mW/cm². The fact that the curve does not fit the Gaussian profile indicates that other factors, including focusing condition, nonlinearity in PEB, and development of SU-8 photoresist, play an important role in the determination of the width of the written lines. In the small feature size or low-intensity region, in particular, the focusing condition is an important issue because it becomes difficult to focus the beam exactly on the surface of the SU-8 resist with the naked eye. We are trying to improve the focusing condition in our updated setup. It can be seen from Fig. 6 that the lower the intensity, the thinner the lines, however, too little exposure can lead to insufficient cross-linkage in the SU-8 resist during PEB to prevent it from dissolving in the developer. Actually, it is difficult for the scanned lines that are less than approximately 3 μm wide to endure the development, but it is easy for them to be kept on the pattern produced by the multiexposures shown below, from which the first three data points in Fig. 6 come from.

From the results shown in Fig. 6, we conclude that, by employing the optical direct-write technique, we can introduce straight lines (and possibly other shapes) into the SU-8 resist, which in turn can be used to produce a line defect in a preexposed 2-D photonic crystal lattice. After the multiple exposures of the sample to rotate the interference patterns as described above, a reflective MO (MO) lens was inserted and adjusted to focus the laser beam on the surface of the resist. The intensity of the direct-write scanning beam was approximately 0.3 mW and the scanning speed was 0.3 cm/s. The exposed sample was baked for 60 at 90 $^{\circ}\text{C}$ and was then developed, rinsed, and observed under the microscope. Figure 7 shows the experimental results on the fabrication of straight-line waveguides consisting of several missing rows of holes in a photonic crystal lattice structure. From observing the large-area image of Fig. 7(a), we conclude that the optical direct write per-

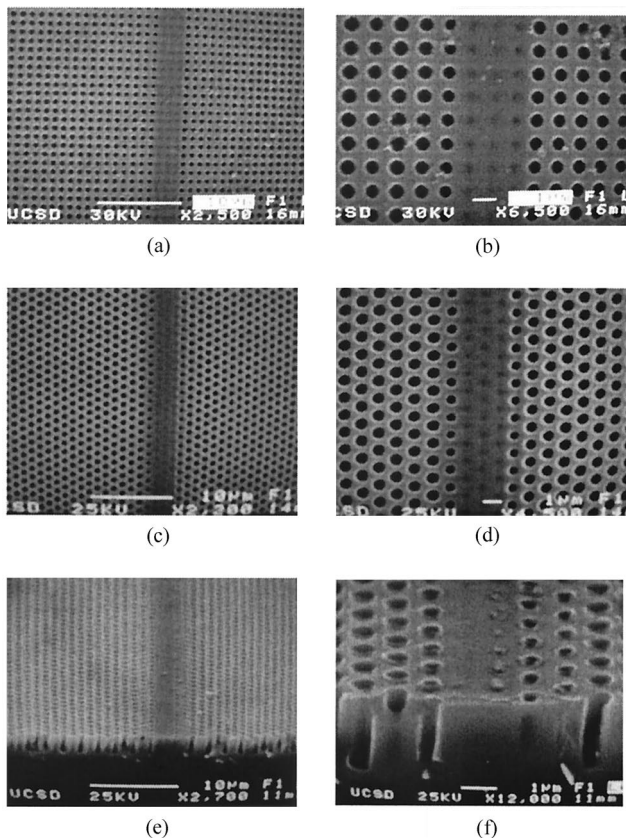


Fig. 7. SEM photographs of (a) a line defect introduced into a rectangular mesh photonic crystal lattice in SU-8; (b) a magnified view of (a) demonstrating the possibility of large-area fabrication with good quality; (c) a line defect introduced into a hexagonal lattice structure with three lines of holes canceled; (d) a magnified view of (c); (e) a line defect transferred into the GaAs substrate with two lines of the hole canceled; (f) a magnified view of (e).

fectly cancels three lines of holes in one dimension and successfully introduces a line defect in the square mesh lattice structure with a period of $1\ \mu\text{m}$. Figure 7(b) shows a magnified view of the introduced defects for the rectangular mesh photonic crystal. Similar results are obtained for the hexagonal mesh photonic crystal lattice with a $1\text{-}\mu\text{m}$ period as shown in Figs. 7(c) and 7(d). As mentioned in subsection 2.C, it is easy to transfer the SU-8 pattern into the GaAs substrate by use of CAIBE as shown in Figs. 7(e) and 7(f). Figure 7(f) shows a magnified view of a waveguide defect introduced into a hexagonal structure lattice with two lines of holes canceled and transferred into GaAs with a $2.1\text{-}\mu\text{m}$ depth. The residue or spots on the surface are due to the incomplete removal of the SU-8 resist after dry-etching or small pieces of GaAs from the cutting of the substrate.

When we look closely at the results of Fig. 7, it appears that two or three rows of holes are eliminated; the adjacent one or two rows of holes also get smaller, which results from the Gaussian distribution of the illumination and the diffusion mechanism of the induced acid during the PEB. It should be possible to minimize the alteration of the adjacent

holes by improving the quality of the focused beam and adjusting the processing of the SU-8 resist.

Another challenge in the optical direct-write technique is the alignment of the scanning direction with the line of holes in the preexposed photonic crystal lattice. Slight misalignment of these two directions will lead to nonuniformity in a number of holes and their shape in the waveguide structure, ruining the periodic nature of the photonic crystal lattice. We used the vertical axis of our optical table to achieve high-precision alignment of the interference pattern to the translation stage axis. For the future we are considering interferometric alignment in an active closed-loop feedback system.

4. Discussion and Conclusion

We have described a novel approach for relatively rapid and easy fabrication of large-area 2-D photonic crystal structures with controlled defects or modifications in the lattice. The technique consists of two lithographic steps. First, the photonic crystal lattice is patterned by use of multiple exposures of a UV-sensitive photoresist with interference fringes at different angles. This results in a square or hexagonal lattice of holes over a large area of the wafer. Then, with a strongly focused beam, additional areas of the pattern are exposed, effectively canceling the holes in the unexposed regions. On the basis of a careful investigation of the exposure properties of the UV photoresist, the set of optical exposures can be calibrated to result in the desired cumulative dosage, and consequently the desired pattern. After development, the CAIBE process is used to transfer the desired pattern into the substrate.

The presented results here are only preliminary, and more improvements are needed to obtain functional devices, including a higher-precision rotation stage, finer control of the focused spot from the MO, and most importantly, minimization of the influence of the exposed waveguides on the adjacent rows of holes. The alteration of the adjacent holes needs to be checked both in measurements and modeling, which we are planning to do next. Also we are attempting to cancel one row of holes in the $0.5\text{-}\mu\text{m}$ period lattice. Although improvements need to be made, this research demonstrates the concept and shows the potential of the technique.

The principal advantage of this approach is the hybrid nature of the lithography process, combining the best features of the existing techniques—quick and easy large-scale patterning of the photonic crystal lattice and high-resolution direct write to introduce controlled modifications. Use of computer-controlled high-precision translation and rotation stages along with incrementally improved optics, significantly more complex alterations to the basic photonic crystal lattice can be realized. Thus we believe that this hybrid optical patterning technique provides a promising opportunity to rapidly and inexpensively implement larger and more complex integrated optical systems based on photonic crystal devices.

This study was supported in part by the National Science Foundation, the Defense Advanced Research Projects Agency, Space and Naval Warfare Systems Command, and the U.S. Air Force Office of Scientific Research.

References

1. A. Blanco, E. Chomski, S. Grabtchak, M. Ibisate, S. John, S. W. Leonard, C. Lopez, F. Meseguer, H. Miguez, J. P. Mondia, G. A. Ozin, O. Toader, and H. M. van Driel, "Large-scale synthesis of a silicon photonic crystal with a complete three-dimensional bandgap near 1.5 micrometers," *Nature (London)* **405**, 437–439 (2000).
2. Y. A. Vlasov, X.-Z. Bo, J. C. Sturm, and D. J. Norris, "On-chip natural assembly of silicon photonic bandgap crystals," *Nature (London)* **414**, 289–293 (2001).
3. M. Campbell, D. N. Sharp, M. T. Harrison, R. G. Denning, and A. J. Turberfield, "Fabrication of photonic crystals for the visible spectrum by holographic lithography," *Nature (London)* **404**, 53–56 (2000).
4. T. Kondo, S. Matsuo, S. Juodkakis, and H. Misawa, "Femtosecond laser interference technique with diffractive beam splitter for fabrication of three-dimensional photonic crystals," *Appl. Phys. Lett.* **79**, 725–727 (2001).
5. S. Shoji and S. Kawata, "Photofabrication of three-dimensional photonic crystals by multibeam laser interference into a photopolymerizable resin," *Appl. Phys. Lett.* **76**, 2668–2670 (2000).
6. V. Berger, O. Gauthie-lafaye, and E. Costard, "Photonic band gaps and holography," *J. Appl. Phys.* **82**, 60–64 (1997).
7. P. Visconti, C. Turco, R. Rinaldi, and R. Cingolani, "Nanopatterning of organic and inorganic materials by holographic lithography and plasma etching," *Microelectron. Eng.* **53**, 391–394 (2000).
8. W. Lee, S. A. Pruzinsky, and P. V. Braun, "Multi-photon polymerization of waveguide structures within three-dimensional photonic crystals," *Adv. Mater.* **14**, 271–274 (2002).
9. O. Painter, R. K. Lee, A. Scherer, A. Yariv, J. D. O'Brien, P. D. Dapkus, and I. Kim, "Two-dimensional photonic band-gap defect mode laser," *Science* **284**, 1819–1821 (1999).
10. M. Loncar, D. Nedeljkovic', T. Doll, J. Vuckovic', A. Scherer, and T. P. Pearsall, "Waveguiding in planar photonic crystals," *Appl. Phys. Lett.* **77**, 1937–1939 (2000).
11. L. Pang, W. Nakagawa, and Y. Fainman, "Fabrication of optical structures using SU-8 photoresist and chemically assisted ion beam etching," *Opt. Eng.* (to be published).
12. K. Y. Lee, N. LaBianca, S. A. Rishton, S. Zolgharnain, J. D. Gelorme, J. Shaw, and T. H.-P. Chang, "Micromachining applications of a high resolution ultrathick photoresist," *J. Vac. Sci. Technol. B* **13**, 3012–3016 (1995).